Polymer Chemistry

Accepted Manuscript

ROYAL SOCIETY OF CHEMISTRY

www.rsc.org/polymers

Polymer Chemistry

RSCPublishing

ARTICLE

Competitive binding-accelerated insulin release from polypeptide nanogel for potential therapy of diabetes†

Cite this: DOI: 10.1039/xoxxooooox

Li Zhao,[a,b] Chunsheng Xiao,[a] Jianxun Ding,[a] Xiuli Zhuang,[a] Guangqing Gai,[b] Liyan Wang[c] and Xuesi Chen*[a]

Received ooth January 2012,
Accepted ooth January 2012

DOI: 10.1039/xoxxooooox

www.rsc.org/

One kind of glucose-sensitive polypeptide nanogel was prepared *via* a two-step procedure. First, methoxy poly(ethylene glycol)-*block*-poly(γ-benzyl-L-glutamate-*co*-(γ-propargyl-L-glutamate-*graft*-glucose) (mPEG-*b*-P(BLG-*co*-(PLG-*g*-Glu))) was synthesized by clicking of 2′-azidoethyl-*O*-α-D-glucopyranoside to the PLG unit in mPEG-*b*-P(BLG-*co*-PLG), which was synthesized by the ring-opening polymerization (ROP) of γ-benzyl-L-glutamate *N*-carboxyanhydride and γ-propargyl-L-glutamate *N*-carboxyanhydride with mPEG-NH_2 as a macroinitiator. And then, the novel kind of nanogel was subsequently prepared by cross-linking the glucose moieties through adipoylamidophenylboronic acid (AAPBA). The formation of nanogel, *i.e.*, the successful incorporation of phenylboronic acid (PBA) in the core, was systematically verified. The resultant nanogel showed remarkable glucose-sensitivity in phosphate-buffered saline (PBS). Thus, insulin as a model drug was loaded into the glucose-sensitive polypeptide nanogel. The *in vitro* drug release profiles revealed that the release of insulin from nanogel could be triggered by the presence of glucose through a competitive binding mechanism with the conjugated glucose. In detail, a faster release rate and a more amount of the releasing insulin were observed by the increased glucose concentration in PBS, which confirmed the potential application of the nanogel. Furthermore, the excellent cytocompatibility and hemocompatibility of the nanogel were demonstrated. Therefore, the biocompatible nanogel with an intelligent capability of glucose-accelerated payload release should be promising for the application in diabetes treatment.

1 Introduction

Diabetes, a chronic disease, becomes one of the three major diseases that endanger human health following cancer and cardiovascular disease, where it is unable for the body to regulate the blood glucose concentration within normal physiological levels.[1] Recently, the total number of peoples with diabetes increases sharply, so the treatment of diabetes is imminent.[2] The frequent administrations of exogenous insulin include injection[3] and non-invasive/non-injectable routes, such as, oral,[4,5] nasal,[6,7] pulmonary,[8,9] and transdermal insulin delivery system.[10,11] For the non-invasive/non-injectable insulin administration, the low bioavailability and other disadvantages limit its wide use for the treatment of diabetes. However, the frequent administration of exogenous insulin by injection every day is not comfortable because of the inevitable pain. In present, the glucose-responsive insulin delivery systems (GRIDSs) are developing rapidly, which are expected to be a promising therapy approach to replace the frequent insulin injection administration. The GRIDSs are practical, which can regulate insulin release continuously and automatically in response to the elevated level of blood glucose for minimizing the intervention toward patient and improving the quality of life.[12]

To develop the GRIDSs, a common strategy is based on the incorporation of glucose oxidase (GOx) with pH-responsive polymeric materials.[13,14] GOx consumes glucose to gluconic acid that grants the pH change of the microenvironment, and thus it causes swelling or shrinking of the carriers incorporated with GOx and leads to the accelerated insulin release in a relatively high glucose level.[15] However, the disadvantages of using enzyme reaction for GRIDSs, such as limited pH and temperature range, and possible bioactivity loss during the preparation of carriers, restrict the potential application in self-regulated insulin release.[16]

Concanavalin A (Con A) is also used for fabricating glucose-sensitive platforms, which is a well-investigated plant lectin protein possessing specific binding capacity with glucose, mannose, and polysaccharide.[17,18] Unfortunately, the instability and biotoxicity of Con A limit its application in GRIDSs.[19]

In contrast, phenylboronic acid (PBA) and its derivatives, known to reversibly form cyclic boronic ester with *cis*-diol compounds, have better potential application in glucose-sensitive insulin delivery due to the better stability and long term storability than GOx and Con A, which are biological molecules and liable to denature.[20–22]

In aqueous solution, the PBA moiety has two forms due to the equilibrium between the neutral trigonal-planar species (marked as PBA_{neu}) and the negatively charged tetrahedral boronate species (noted as PBA_{neg}). The PBA_{neu} is relative hydrophobic (pH < pK_a of PBA, ~ 8.2),[23] while the PBA_{neg} is relative hydrophilic (pH > pK_a of PBA). Both the two structures can form complexes with diols. However, only the PBA_{neg} can form the stable cyclic boronic ester with *cis*-diol compounds, which makes the equilibrium shift to the

negatively charged form and improves the hydrophilicity of PBA-functionalized materials.[24,25] Glucose bearing *cis*-diol groups is well-documented to form stable glucose-PBA complex at neutral or alkaline pH. When PBA or its derivatives are immobilized in the drug delivery matrices, the presence of glucose can induce the swelling of platforms and subsequent release of the payload *via* the formation of hydrophilic glucose-PBA complex.[26,27] However, the further practical application is limited by the unbiodegradable materials, such as poly(acrylic acid) polymers[28–32] and silica-based materials,[33,34] which incorporate PBA used for mostly GRIDSs.

Synthetic polypeptides are one of the most important biocompatible and biodegradable polymers, which have been widely studied for various biomedical applications, such as, drug and gene delivery,[35–39] antibacterial materials,[40,41] and tissue engineering.[42,43] However, polypeptides have rarely been used as drug-loaded materials for GRIDSs.[27,44] In this work, the glucose-sensitive nanogel was prepared by crosslinking glycopolypeptide using adipoylamidophenylboronic acid (AAPBA). Insulin, a model drug, was loaded into the glucose-sensitive polypeptide nanogel, and the drug release behaviors triggered by glucose at physiological pH were studied. Moreover, the biocompatibility of nanogel was also confirmed.

2 Experimental section

2.1 Materials

γ-Benzyl-L-glutamate *N*-carboxyanhydride (BLG NCA), γ-propargyl-L-glutamate *N*-carboxyanhydride (PLG NCA), and 2′-azidoethyl-*O*-α-D-glucopyranoside were similarly synthesized as our previous works.[27,39,45] D-(+)-Glucose (99%) was purchased from Alfa Aesar (Shanghai, P. R. China) and used as received. Methoxy poly(ethylene glycol) (mPEG, number average molecular weight (M_n) = 5,000 Da) was purchased from Sigma-Aldrich (Shanghai, P. R. China) and used without further purification. The amino-terminated mPEG (*i.e.*, mPEG-NH_2) was synthesized according to the literature procedure.[46] 3-Aminophenylboronic acid (APBA), *N*-(3-dimethylaminopropyl)-*N*-ethyl-carbodiimide hydrochloride (EDC·HCl), *N*-hydroxysuccinimide (NHS), and insulin (bovine pancreas, > 27 IU mg^{-1}, Sigma-I5500) were purchased from Sigma-Aldrich (Shanghai, P. R. China). *N*,*N*′,*N*″,*N*‴-Pentamethyldiethylenetriamine (PMDETA) and cuprous bromide (CuBr) (99.99%) were purchased from Aladdin Reagent Co., Ltd., Shanghai, P. R. China. *N*,*N*-Dimetylformamide (DMF) and dimethyl sulfoxide (DMSO) were stored over calcium hydride (CaH_2) and purified by vacuum distillation.

2.2 Preparation of nanogel

2.2.1 Synthesis of methoxy poly(ethylene glycol)-*block*-poly(γ-benzyl-L-glutamate-*co*-(γ-propargyl-L-glutamate) (mPEG-*b*-P(BLG-*co*-PLG)). mPEG-*b*-P(BLG-*co*-PLG) was synthesized by the ring-opening polymerization (ROP) of BLG NCA and PLG NCA using mPEG-NH_2 as a macroinitiator. Typically, mPEG-NH_2 (1.04 g, 0.21 mmol) was dissolved in 25.0 mL of dry DMF in a flame-dry flask, and then BLG NCA (1.64 g, 6.24 mmol) and PLG NCA (1.32 g, 6.24 mmol) solution in 100.0 mL of dry DMF was added under vigorously stirring. After stirring for 3 days at 25 °C, the excess solvent was removed under reduced pressure. The resultant mPEG-*b*-P(BLG-*co*-PLG) was dissolved in 30.0 mL of chloroform and precipitated into excessive diethyl ether. The obtained product was further washed twice with diethyl ether and dried under vacuum to a constant weight at room temperature, affording 85.6% yield, $M_{n,\,NMR}$ = 15800 g mol^{-1}, $M_{n,\,GPC}$ = 12700 g mol^{-1}, and M_w/M_n = 1.63. Proton nuclear magnetic resonance (^{1}H NMR, DMSO-d_6): δ = 5.06 ppm ($C_6H_5CH_2$−, 2H), 4.65 ppm (CH≡CCH_2−, 2H), 3.92 − 4.21 ppm (−C(O)CH(CH_2−)NH−, 1H), 3.52 ppm (−CH_2CH_2O−, 4H), and 1.78 − 2.38 ppm (−C(O)CH_2CH_2−, 4H, and CH≡CCH_2−, 1H).

2.2.2 Synthesis of methoxy poly(ethylene glycol)-*block*-poly(γ-benzyl-L-glutamate-*co*-(γ-propargyl-L-glutamate-*graft*-glucose) (mPEG-*b*-P(BLG-*co*-(PLG-*g*-Glu))). The glycopolypeptide mPEG-*b*-P(BLG-*co*-(PLG-*g*-Glu)) was synthesized by clicking 2′-azidoethyl-*O*-α-D-glucopyranoside to the PLG unit in mPEG-*b*-P(BLG-*co*-PLG). Briefly, 0.39 g of mPEG-*b*-P(BLG-*co*-PLG) containing about 0.69 mmol alkyne pendants, 0.19 g of 2′-azidoethyl-*O*-α-D-glucopyranoside (1.1 equivalent of alkyne pendants), and 14.5 μL of PMDETA (about 0.07 mmol) were dissolved in 30.0 mL of DMF. Oxygen was removed from the solution by three freeze-pump-thaw cycles. CuBr (0.01 g, 0.07 mmol) was quickly added into the frozen solution, and the flask was reevacuated, backfilled with nitrogen, and sealed. The reaction mixture was stirred at room temperature for 3 days, and then 150.0 mg of Dowex HCR-W2 resins (Sigma-Aldrich) were added and stirred at room temperature over night to remove the copper ions. After filtrating out the resins, the solution was dialyzed against deionized water for 3 days using a dialysis bag (molecular weight cut-off (MWCO) = 7,000 Da) and then lyophilized. Yield: 69.1%, $M_{n,\,NMR}$ = 22700 g mol^{-1}, $M_{n,\,GPC}$ = 13500 g mol^{-1}, and M_w/M_n = 1.66. Proton nuclear magnetic resonance (^{1}H NMR, DMSO-d_6): δ = 5.06 ppm ($C_6H_5CH_2$−, 2H), 4.65 ppm (CH≡CCH_2−, 2H), 3.67 − 4.21 ppm (−C(O)CH(CH_2−)NH−, 1H, and hydroxyl groups from glucose), 3.52 ppm (−CH_2CH_2O−, 4H), 2.95 – 3.12 ppm ($C_6H_{12}O_6CH_2$−CH_2−, 4H, and hydroxyl groups from glucose), and 1.78 − 2.38 ppm (−C(O)CH_2CH_2−, 4H).

2.2.3 Synthesis of AAPBA. AAPBA was prepared simply through the condensation reaction as the following description. Briefly, 1.86 g of APBA (10.93 mmol, 2.2 equiv) was dissolved in 25.0 mL of pyridine, and the solution was incubated in ice bath, to which 0.79 mL of adipoyl chloride (5.46 mmol) was added drop by drop. The final solution was stirred at room temperature for 24 h. Then, 120.0 mL of deionized water was added into the solution to yield the little yellow solid precipitate. After three times washing with deionized water, the precipitate was collected and recrystallized in ethanol/water (1:1, V/V) at 65 °C. The final product AAPBA was dried under vacuum to a constant at room temperature and obtained as a white solid (Yield: 85.5 %). Proton nuclear magnetic resonance (^{1}H NMR, DMSO-d_6): δ = 1.62 ppm (dd, −C(O)CH_2CH_2−, 2H), 2.32 ppm (dd, −C(O)C$H_2$$CH_2$−, 2H), 7.21 − 7.82 ppm (dd, d, d, s, ArH, 1H each), 7.99 ppm (s, $B(OH)_2$, 2H), and 9.82 ppm (s, NH, 1H). The ^{1}H NMR spectrum of AAPBA was shown in Fig. S1, ESI†.

2.2.4 Preparation of nanogel. The nanogel was prepared by cross-linking of mPEG-*b*-P(BLG-*co*-(PLG-*g*-Glu)) with AAPBA *via* the formation of boronic ester. Briefly, 60.0 mg of mPEG-*b*-P(BLG-*co*-PLG-Glu) (about 0.074 mmol glucose pendants) and 17.2 mg of AAPBA (1.1 equivalent of glucose pendants) were dissolved in 3.0 mL of DMSO. And then, the solution was stirred overnight before 1.0 mL of deionized water was added slowly. The mixture was further stirred for about 12 h, and then filtered and dialyzed against deionized water for 2 days using a dialysis bag (MWCO = 7,000 Da). The final nanogel was obtained as a white spongy solid by lyophilization (Yield: 59.1 %).

2.3 Characterizations

^{1}H NMR spectra were recorded on a Bruker AV 400 NMR spectrometer in DMSO-d_6. The molecular weight distributions (M_w/M_n) were determined by gel permeation chromatography (GPC) equipped with Waters 515 HPLC pump, and Waters Styragel HT3

and HT4 columns. DAWN EOS 18 Angles Laser Light Scattering Instructment (Wyatt Technology) and OPTILAB DSP Interferometric Refractometer (Wyatt Technology) were used as the detectors. The eluent was DMF containing 0.01M lithium bromide (LiBr) at a flow rate of 1.0 mL min^{-1} at 40 °C. Fourier-transform infrared (FT-IR) spectra were recorded on a Bio-Rad Win-IR instrument using potassium bromide method. Transmission electron microscopy (TEM) measurements were performed on a JEOL JEM-1011 transmission electron microscope with an accelerating voltage of 100 kV. To prepare the TEM samples, a small drop of the nanogel solution (0.10 mg mL^{-1} in deionized water) was deposited onto a 230 mesh copper grid coated with carbon and allowed to dry at 25 °C before measurements. Dynamic laser scattering (DLS) measurements were performed on a WyattQELS instrument with a vertically polarized He-Ne laser (DAWN EOS, Wyatt Technology) at a collecting optics of 90°. All samples were prepared in aqueous solution with a concentration of 0.10 mg mL^{-1}, and measurements were carried out at 25 °C. Each sample was kept in the thermostat for 30 min prior to measurements.

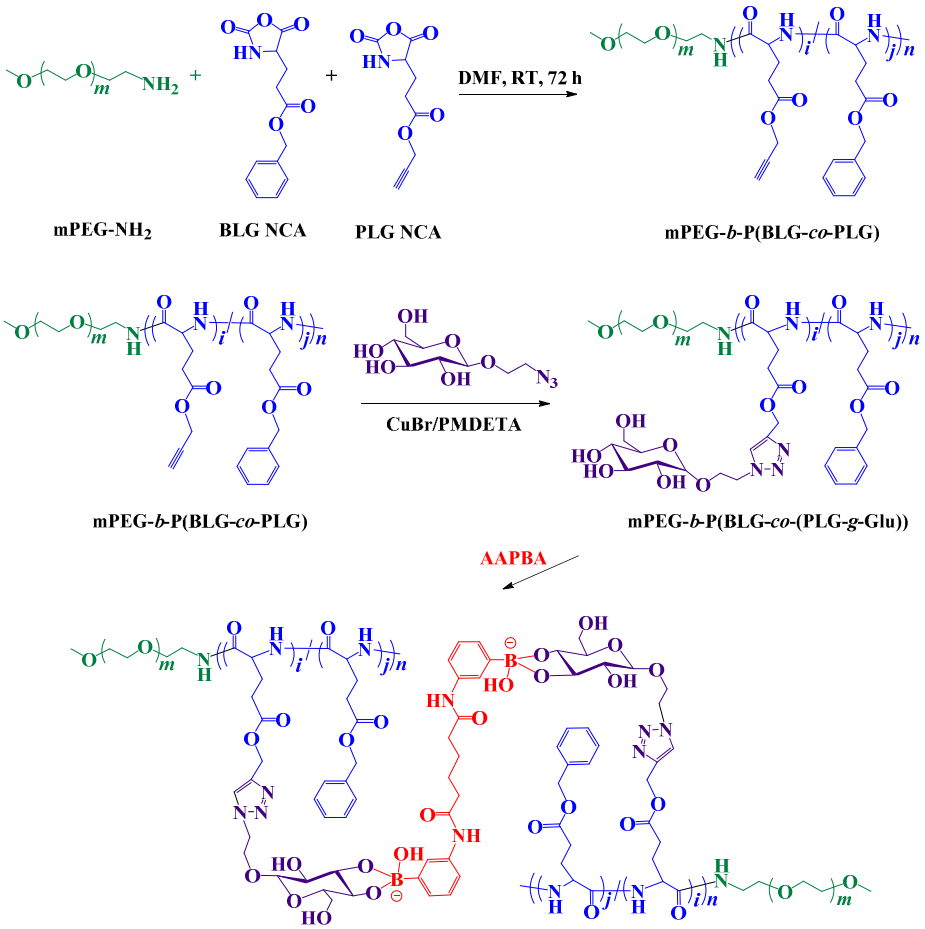

Scheme 1. Synthetic pathway for glucose-sensitive nanogel.

2.4 *In vitro* insulin loading and release

The insulin-loaded nanogel was prepared similarly as the preparation of nanogel. The difference was that 1.0 mL of insulin aqueous solution (16.0 mg insulin) substituting 1.0 mL of deionized water was added into the solution of mPEG-*b*-P(BLG-*co*-(PLG-*g*-Glu)) and AAPBA. The insulin-loaded nanogel was obtained as a white flocculent solid by lyophilization. The entrapment capacity (EC) and entrapment efficiency (EE) were calculated by Equations (1) and (2):

$$\text{EC (wt. \%)} = \frac{\text{amount of insulin in nanogel}}{\text{amount of insulin-loaded nanogel}} \times 100\% \quad (1)$$

$$\text{EE (wt. \%)} = \frac{\text{amount of insulin in nanogel}}{\text{total amount of feeding insulin}} \times 100\% \quad (2)$$

In vitro insulin release from the insulin-loaded nanogel was evaluated in PBS at pH 7.4 with different glucose concentrations (0, 0.5, 1.0, 2.0, and 3.0 mg mL^{-1}). Typically, 5.0 mg of insulin-loaded nanogel was first dispersed in 3.0 mL of PBS and subsequently introduced into a dialysis bag (MWCO = 7,000 Da). The release experiment was initiated by placing the end-sealed dialysis bag into 10.0 mL of PBS at 37 °C with continuous shaking at 70 rpm. Aliquot of dissolution medium was taken out at predetermined time-point, and isometric fresh release medium was added. The insulin amount was determined by the bicinchoninic acid protein assay. All the release experiments were carried out in triplicate, and the results were reported as mean ± standard deviation.

2.5 Circular dichroism (CD) measurements

The stability of the releasing insulin was also determined by comparing the conformation with standard insulin. The free insulin solution with the concentration of 0.2 mg mL^{-1} was prepared in PBS at pH 7.4. CD measurements were performed on a MOS-450 CD spectrophotometer (France Biologic Company, Grenoble, France) at 25 °C with a cell length of 0.1 cm. For the CD spectra, samples were scanned from 190 to 260 nm with the scanning speed of 1 nm/20 s. All CD data were expressed as mean residue ellipticity.

2.6 MTT assays

The cytotoxicities of copolymers and nanogel were assessed through a methyl thiazolyl tetrazolium (MTT) viability assay against HeLa cells as our previous works.[26, 27] Polyethyleneimine with weight-average molecular weight (M_w) of 25 kDa (PEI25k) and AAPBA were used as positive controls. The cells were plated in 96-well plates at 7,000 cells per well in 200.0 μL of complete Dulbecco's modified Eagle's medium (DMEM) containing 10% (V/V) fetal bovine serum, supplemented with 50.0 IU mL^{-1} penicillin and 50.0 IU mL^{-1} streptomycin, and incubated at 37 °C in 5% (V/V) carbon dioxide atmosphere for 24 h. At the following day, the medium was removed and the cells were treated with the solutions of copolymers and nanogel in 200.0 μL of complete DMEM with the concentrations from 0 to 0.1 mg mL^{-1}. After 72 h incubation, 20.0 μL of MTT stock solution (5.0 mg mL^{-1} in PBS) was added into each well to achieve a final concentration at 0.5 mg mL^{-1}. The cells were subjected to MTT assay after being incubated for another 4 h. The absorbance of the solution was measured on a Bio-Rad 680 microplate reader at 490 nm. Cell viability was calculated based on the equation (3):

$$\text{Cell viability (\%)} = \frac{A_{\text{sample}}}{A_{\text{control}}} \times 100\% \quad (3)$$

Where, A_{sample} and A_{control} were denoted as the absorbances of sample and control wells, respectively.

2.7 Hemolysis activity tests

The blood compatibility of nanogel was examined by spectrophotometry technique.[47] The Experimental Animal Center of Jilin University supervised the experiments and offered the dipotassium ethylene diamine tetraacetate (K_2EDTA)-stabilized rabbit blood. First, 5.0 mL of blood sample was added into 10.0 mL of physiological saline, and then red blood cells (RBCs) were isolated from serum by centrifugation at 1200 *g* for 8 min. The RBCs were further washed five times with 10.0 mL of physiological saline. The purified blood was diluted to 50.0 mL by physiological saline. Then, 0.4 mL of diluted RBC suspension was added into 0.4 mL of mPEG-*b*-P(BLG-*co*-PLG), mPEG-*b*-P(BLG-*co*-(PLG-*g*-Glu)), nanogel, and AAPBA at systematically varied concentrations and mixed by vortexing. Herein, RBCs incubated with physiological saline (−) and Triton X-100 (10.0 mg mL^{-1}) (+) were used as negative and positive controls, respectively. All the sample tubes were kept in static condition at 37 °C for 1 h. Finally, the mixtures were centrifuged at 3000 *g* for 10 min, and 100.0 μL of the supernatant of all samples was transferred into a 96-well plate. The absorbance values of the supernatants at 540 nm were determined by a Bio-Rad 680 microplate reader. The hemolysis ratio (HR) of RBCs was calculated using the Equation (4):

$$\text{HR (\%)} = \frac{A_{\text{sample}} - A_{\text{negative control}}}{A_{\text{positive control}} - A_{\text{negative control}}} \times 100\% \quad (4)$$

Where, A_{sample}, $A_{\text{negitive control}}$, and $A_{\text{positive control}}$ were denoted as the absorbances of sample, negative, and positive controls, respectively.

3 Results and discussion

3.1 Synthesis and characterization of glucose-sensitive nanogel

PBA and its derivatives that can reversibly interact with diols have been widely utilized as glucose sensors or in GRIDSs.[48,49] In this work, the biocompatible glucose-sensitive nanogel was prepared by cross-linking mPEG-*b*-P(BLG-*co*-(PLG-*g*-Glu)) with AAPBA. mPEG-*b*-P(BLG-*co*-(PLG-*g*-Glu)) was prepared through a two-step procedure. First, mPEG-*b*-P(BLG-*co*-PLG) was first synthesized by the ROP of BLG NCA and PLG NCA using mPEG-NH_2 as a macroinitiator. The azido-functionalized glucose was coupled with PLG unit by clicking reaction to afford mPEG-*b*-P(BLG-*co*-(PLG-*g*-Glu)) (Scheme 1). The chemical structures of block copolymers were confirmed by ^{1}H NMR and FT-IR spectra. As shown in Fig. 1a, the representative spectrum of mPEG-*b*-P(BLG-*co*-PLG) was characterized as follows (δ, ppm): 5.06 ppm (f, $C_6H_5CH_2$−, 2H), 4.65 ppm (e, CH≡CCH_2−, 2H), 3.92 − 4.21 ppm (b + c, −C(O)C*H*(CH_2−)NH−, 1H), 3.52 ppm (a, −CH_2CH_2O−, 4H), and 1.78 − 2.38 ppm (d, −C(O)CH_2CH_2−, 4H, and g, C*H*≡CCH_2−, 1H). The DP of both BLG and PLG blocks was calculated to be 28 based on the intensities of methylene group in mPEG (−CH_2CH_2O−, 3.52 ppm) and those in the pendent groups of P(BLG-*co*-PLG) at 5.06 ppm (f, $C_6H_5CH_2$−, 2H) and 4.65 ppm (e, CH≡CCH_2−, 2H), respectively. The mPEG-*b*-P(BLG-*co*-(PLG-*g*-Glu)) copolymer was prepared by clicking reaction between azido-functionalized glucose and PLG unit. The ^{1}H NMR spectrum was shown in Fig. 1b and revealed new signals at 2.95 − 3.12 and 3.67 − 4.21 ppm, which were attributed to the glucose and indicated the successful preparation of glycopolypeptides, that is, mPEG-*b*-P(BLG-*co*-(PLG-*g*-Glu)).

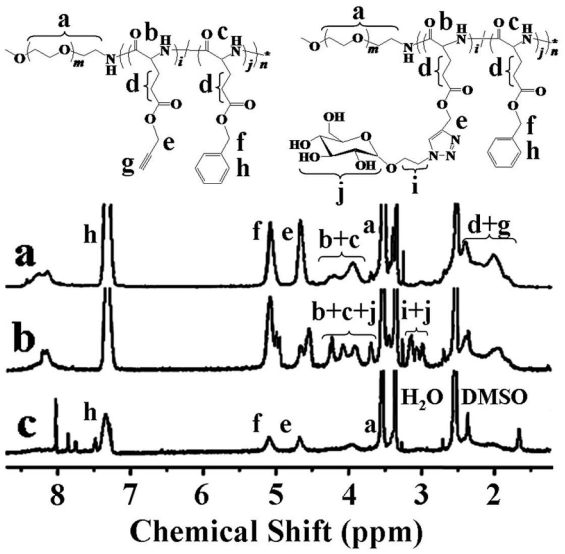

Fig. 1 ^{1}H NMR spectra of mPEG-*b*-P(BLG-*co*-PLG) (a), mPEG-*b*-P(BLG-*co*-(PLG-*g*-Glu)) (b), and nanogel (c) in DMSO-d_6.

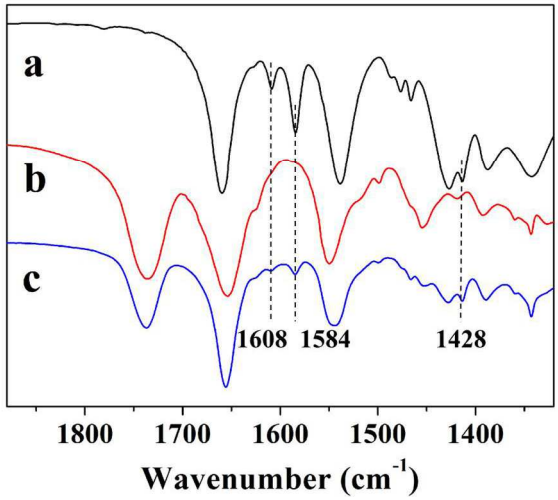

Fig. 2 FT-IR spectra of AAPBA (a), mPEG-*b*-P(BLG-*co*-(PLG-*g*-Glu)) (b), and nanogel (c).

Subsequently, nanogel was successfully prepared by cross-linking with boronic ester bond using AAPBA as a cross-linker (Scheme 1). As shown in Fig. 1c, the signals from the glucose and the pendent groups of copolymer weakened or even disappeared, while the new signals at 7.5 − 8.0 ppm appeared from AAPBA. It indicated that the nanogel was prepared successfully by incorporating AAPBA with the glucose moieties. FT-IR spectra were further employed to characterize the copolymers and nanogel (Fig. 2). The typical absorption bands of the phenyl ring in AAPBA at 1428, 1584, and 1608 cm^{-1} in the nanogel implied that AAPBA as cross-linker was successfully introduced into the core of nanogel.[50–53]

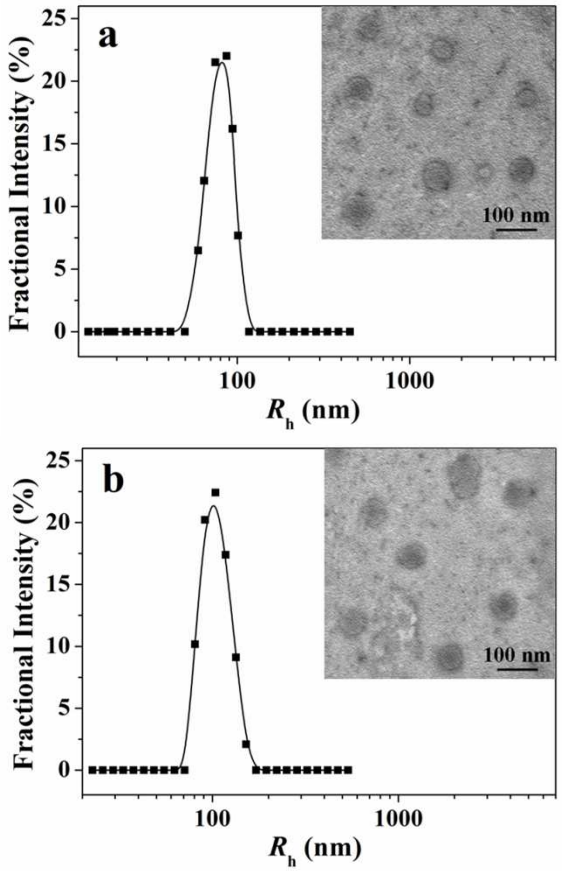

Fig. 3 R_hs and distributions of nanogel (a) and insulin-loaded nanogel (b). The inset microimages were the typical TEM micrographs of corresponding nanogels.

The hydrodynamic radius (R_h) of nanogel was characterized to be 84.7 ± 1.5 nm (polydispersity index (PDI) = 0.12) in PBS by DLS technique (Fig. 3a). TEM observation indicated that the nanogel was spherical with an average diameter of about 65 ± 7.0 nm (Fig. 3a, inset). The smaller size of nanogel from TEM observation should be attributed to the collapse of nanogel in the preparation process of TEM sample. In addition, the nanogel was demonstrated to have excellent stability in aqueous solution. As shown in Fig. S2, ESI†, the size of the nanogel did not change as its concentration decrease. The R_h of nanogel at 25 °C was same as that at 37 °C owing to the fact that there was no thermo-sensitive segment in nanogel (data was not shown). The R_h of nanogel in DMF was 106 ± 6.0 nm (PDI = 0.13), which was larger than that in PBS at pH 7.4 due to the swelling of nanogel core in DMF (Fig. S3, ESI†).

3.2 Glucose-sensitivity of nanogel

AAPBA incorporated in the core of nanogel endowed them with good glucose-sensitivity. Fig. 4a shows the R_h variation of nanogel in PBS with different glucose concentrations. With the increase of glucose concentration from 0 to 1.0 mg mL^{-1}, the R_h of nanogel kept a slow growth of size from 84.7 ± 1.5 (PDI = 0.12) to 87 ± 1.9 nm (PDI = 0.11). Upon the glucose concentration increasing from 1.0 to 3.0 mg mL^{-1}, the R_h showed a rapid growth. The swelling phenomenon was induced by the structure of nanogel, which could be influenced by free glucose in the solution. In details, at a higher glucose concentration, more free glucose molecules entered into the core resulting in the swelling of nanogel. Moreover, more free glucose molecules formed the complexes with PBA, which destroyed the cross-linking and endowed the nanogel with more hydrophilicity resulting in the increase of nanogel size. When the glucose concentration was above 3.5 mg mL^{-1}, the nanogel exhibited the largest expansion with R_h at 111.5 ± 1.7 nm (PDI = 0.10). The result should be attributed to the dissociation of nanogel in a higher glucose concentration. Fig. 4b shows the size distributions of nanogel at various glucose concentrations. As description, the R_h increased clearly, and the size distributions became much larger with the increase of glucose concentration. Furthermore, TEM measurement was employed to confirm the size change of nanogel. As shown in Fig. S4, ESI†, the average diameter of nanogel was about 85 ± 7.3 nm in PBS at pH 7.4 with 3.0 mg mL^{-1} of glucose, which was much larger than that in PBS without the addition of glucose (65 nm) indicating the excellent glucose-sensitivity of nanogel.

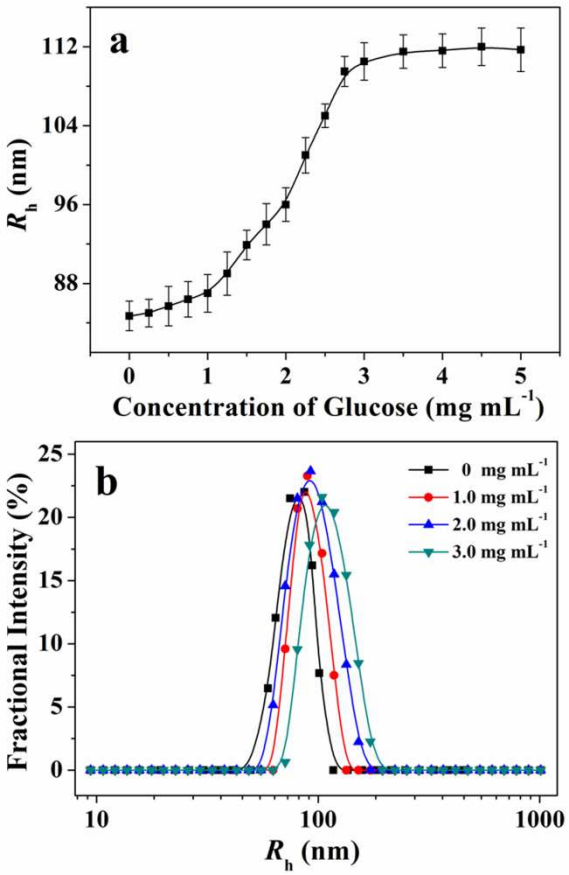

Fig. 4 R_h of nanogel as a function of glucose concentration in PBS at pH 7.4 (a), and size distributions of nanogel in different glucose concentrations (b).

3.3 *In vitro* insulin loading and release

The successful fabrication of nanogel with great glucose-sensitivity provided a good basis to study the drug loading and release behaviors. The release behaviors of insulin-loaded nanogel were investigated in PBS with the presence of glucose at different concentrations. Insulin could be entrapped into the nanogel during the formation process with the EC and EE of the insulin-loaded nanogel at 9.5 and 47.5 wt.%, respectively. The R_h and morphology of the insulin-loaded nanogel were shown in Fig. 3b. The R_h of insulin-loaded nanogel was 105 ± 4.5 nm (PDI = 0.11), which was much larger than that without insulin (Fig. 3), indicating the efficient incorporation of insulin into nanogel. TEM micrograph further demonstrated that the insulin-loaded nanogel still exhibited the spherical morphology with a narrow size distribution and an average diameter of 74.1 ± 6.0 nm (PDI = 0.12; Fig. 3b, inset).

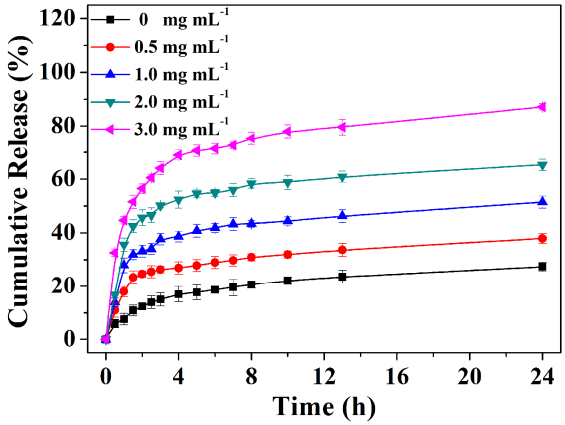

Fig. 5 Cumulative insulin release from insulin-loaded nanogel in PBS with various glucose concentrations at pH 7.4, 37 °C. Each datum was represented the average of three independent determinations.

As shown in Fig. 5, the release of insulin was also confirmed to be glucose-sensitive. As expected, the release of insulin increased with increasing glucose concentration. For all cases, there was a fast initial release because some insulin was entrapped on the surface of nanogel. At the first 2 h, the release profile exhibited a fast release at all examined glucose concentrations, and 12.3, 24.6, 33.2, 45.7, and 56.5% of insulin released in PBS containing 0, 0.5, 1.0, 2.0, and 3.0 mg mL^{-1} glucose, respectively. The cumulative amount of insulin had a slight increase after 2 h in PBS without glucose because the insulin was tightly wrapped in the hydrophobic core of nanogel through the hydrophobic, electrostatic, and/or hydrogen bonding interactions between the core of nanogel and insulin molecule.[54]

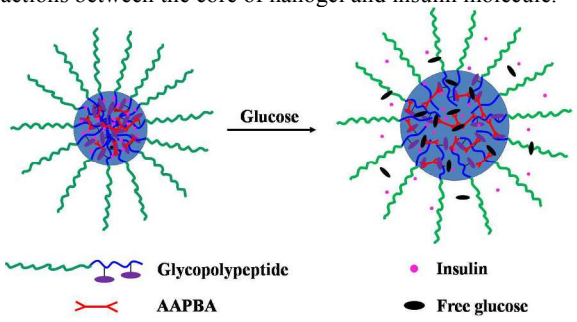

Scheme 2 Glucose-responsive insulin release from PBA-functionalized polypeptide nanogel.

Furthermore, as the more glucose molecules were added into the medium, the more insulin agents released from the nanogel. With 1.0 mg mL^{-1} of glucose, that is, the preprandial blood glucose level in healthy human body, 51.5% of insulin released after 24 h. In contrast, 65.3 and 87.2% of insulin released in the glucose solution of 2.0 and 3.0 mg mL^{-1}, respectively, given that the prandial blood glucose concentration for diabetics is above 2.0 mg mL^{-1}. As shown in Scheme 2, with the increase of glucose concentration in the medium, more glucose entered the nanogel and bound with PBA. It resulted in the swelling of nanogel and more release of insulin. Furthermore, the release of insulin from the nanogel was accelerated by the high glucose concentration equal to or above 2.0 mg mL^{-1} (*i.e.*, the blood glucose level of diabetics), indicating the potential application of nanogel as a glucose-sensitive delivery vehicle for the treatment of diabetes.

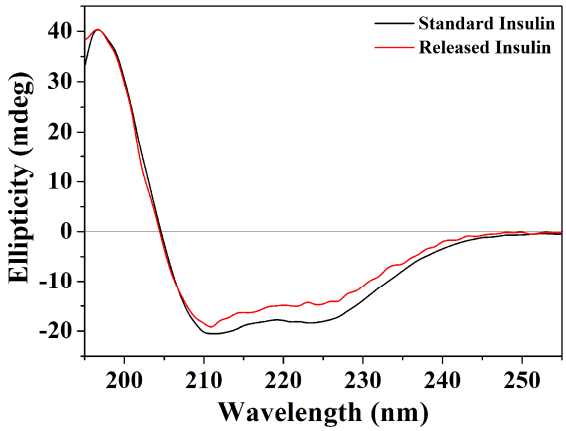

Fig. 6 CD spectra of releasing insulin and standard insulin in PBS at pH 7.4, 25 °C.

One critical demand for the insulin delivery system is to preserve the bioactivity of releasing insulin. Herein, to confirm the bioactivity of releasing insulin, CD spectroscopy was used to determine the conformation of insulin after its release from the nanogel.[55] As shown in Fig. 6, no significant difference in CD spectra was observed between the releasing insulin and standard insulin, indicating that the secondary structure of insulin was undistorted after release from the nanogel. In other words, the insulin releasing from the nanogel substantially maintained the original bioactivity.

3.4 *In vitro* biocompatibility of nanogel

In this work, the *in vitro* cytotoxicity of nanogel toward HeLa cells was evaluated by a MTT assay. The cells were treated with nanogel at different concentrations for 72 h using PEI25k and AAPBA as positive controls. It was observed that the viability of HeLa cells treated with nanogel was above 95% at all test concentrations up to 0.1 mg mL^{-1} (Fig. S5, ESI†), indicating the low cytotoxicity and good compatibility of nanogel.

The blood compatibility of nanogel was assessed by a hemolysis assay. The HR represents the degree of RBC membranes destroyed by the substance in contact with blood. A smaller HR value represents better hemocompatibility of biomaterials. RBCs were coincubated with the nanogel at different concentrations for 1 h, and then the test results were visually sorted out (Fig. 7a), and HR values were determined with spectrophotometer (Fig. 7b). As shown in Fig. 7, the nanogel did not show conspicuous hemolytic activity against RBCs even at a high concentration of 1.0 mg mL^{-1}, indicating that the nanogel was hemocompatible for potential biomedical application. All the above results confirmed that the glucose-sensitive nanogel was biocompatible for promising biomedical applications.

4 Conclusions

A novel kind of nanogel was prepared by the ROP of BLG NCA and PLG NCA using mPEG-NH_2 as a macroinitiator followed by clicking of azido-modified glucose to the PLG unit and subsequent

cross-linking with AAPBA. The resultant spherical nanogel showed remarkable glucose-sensitivity in PBS. The gradual increasing of R_h from 84.7 ± 1.5 to 110.5 ± 1.9 nm was observed as the glucose concentration increased from 0 to 3.0 mg mL^{-1}. The *in vitro* release results revealed that the release of insulin from the nanogel was highly dependent on the glucose concentration, *i.e.*, a higher release rate and a more amount of releasing insulin were achieved by increasing the glucose concentration in PBS. Additionally, the nanogel was demonstrated to be non-toxic. Therefore, the biocompatible nanogel with intelligent glucose-triggered drug release ability should be promising in self-regulated drug delivery for the therapeutic of diabetes.

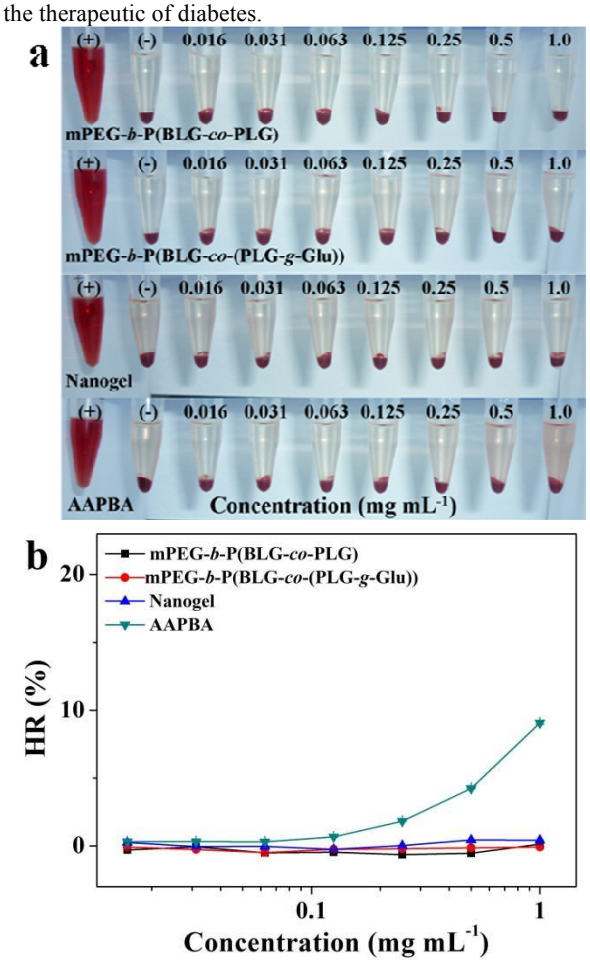

Fig. 7 Photographs (a) and percentages of RBC hemolysis (b) in the presence of copolymers, nanogel, and AAPBA. Physiological saline (−) and Triton X-100 (10.0 mg mL^{-1}) (+) were used as negative and positive controls, respectively. Data were represented as mean ± standard deviation from three independent experiments.

Acknowledgements

This work was financially supported by National Natural Science Foundation of China (51403075, 51303174, 51203153, 51273196, 51233004, and 51321062), the Ministry of Science and Technology of China (2011DFR51090), and the Scientific Development Program of Jilin Province (20140520050JH, 201215175, and 20125059), the Research and Development Project of Ministry of Housing and Urban–Rural Development (2014-K1-020), and the Science and Technology Planning Project of Changchun City (14KG079 and 13KG70).

Notes and references

[a] *Key Laboratory of Polymer Ecomaterials, Changchun Institute of Applied Chemistry, Chinese Academy of Sciences, Changchun 130022, P. R. China. E-mail: xschen@ciac.ac.cn; Tel./Fax: +86 431 8526-2112*
[b] *Laboratory of Building Energy-Saving Technology Engineering, Jilin Jianzhu University, Changchun 130118, P. R. China*
[c] *College of Material Science and Engineering, Jilin Jianzhu University, Changchun 130118, P. R. China*

† Electronic Supplementary Information (ESI) available. See DOI: 10.1039/ x0xx00000x.

1 C. Valeri, P. Pozzilli and D. Leslie, *Diabete-Metab. Res. Reviews*, 2004, **20**, S1–S8.
2 S. Wild, G. Roglic, A. Green, R. Sicree and H. King, *Diabetes Care*, 2004, **27**, 1047–1053.
3 D. H. Bell, *Drugs*, 2007, **67**, 1813–1827.
4 H. Iyer, A. Khedkar and M. Verma, *Diabetes Obes. Metab.*, 2010, **12**, 179–185.
5 P. Mukhopadhyay, R. Mishra, D. Rana and P. P. Kundu, *Prog. Polym. Sci.*, 2012, **37**, 1457–1475.
6 A. C. Sintov, H. V. Levy and S. Botner, *J. Control. Release*, 2010, **148**, 168–176.
7 S. Soares, A. Costa and B. Sarmento, *Expert Opin. Drug Deliv.*, 2012, **9**, 1539–1558.
8 F. Fang, Y. Lu, Y. Liang, J. Zhu, J. K. He, J. H. Zheng, N. Li, Y. Tang, J. B. Zhu and X. J. Chen, *Pharmazie*, 2012, **67**, 706–711.
9 T. K. Mandal, *Am. J. Health, Syst. Pharm.*, 2005, **62**, 1359–1364.
10 Y. Tahara, S. Honda, N. Kamiya and M. Goto, *Med. Chem. Comm.*, 2012, **3**, 1496–1499.
11 Y. Ito, T. Nakahigashi, N. Yoshimoto, Y. Ueda, N. Hamasaki and K. Takada, *Diabetes Technol. Ther.*, 2012, **14**, 891–899.
12 Q. Wu, L. Wang, H. Yu, J. Wang and Z. Chen, *Chem. Rev.*, 2011, **111**, 7855–7875.
13 R. M. Luo and H. Li, *Soft Mater.*, 2013, **11**, 69–74.
14 J. Luo, S. Q. Cao, X. Y. Chen, S. N. Liu, H. Tan, W. Wu and J. S. Li, *Biomaterials*, 2012, **33**, 8733–8742.
15 W. Zhao, H. Zhang, Q. He, Y. Li, J. Gu, L. Li, H. Li and J. Shi, *Chem. Commun.*, 2011, **47**, 9459–9461.
16 M. Samoszuk, D. Ehrlich and E. Ramzi, *J. Pharmacol. Exp. Ther.*, 1993, **266**, 1643–1648.
17 M. J. Taylor, S. Tanna, T. S. Sahota and B. Voermans, *Eur. Pharm. Biopharm.*, 2006, **62**, 94–100.
18 S. Tanna, T. S. Sahota, K. Sawicka and M. J. Taylor, *Biomaterials*, 2006, **27**, 4498–4507.
19 R. Ballerstadt, C. Evans, R. McNichols and A. Gowda, *Biosensors Bioelectron*, 2006, **22**, 275–284.
20 R. Nishiyabu, Y. Kubo, T. D. James and J. S. Fossey, *Chem. Commun.*, 2011, **47**, 1124–1150.
21 V. Ravaine, V. Lapeyre, I. Gosse and S. Chevreux, *Biomacromolecules*, 2006, **7**, 3356–3363.
22 T. D. James, K. R. A. S. Sandanayake and S. Shinkai, *Angew. Chem.*, 1996, **108**, 2038–2050.
23 A. Matsumoto, S. Ikeda, A. Harada and K. Kataoka, *Biomacromolecules*, 2003, **4**, 1410–1416.

24 A. Matsumoto, K. Yamamoto, R. Yoshida, K. Kataoka, T. Aoyagi and Y. Miyahara, *Chem. Commun.*, 2010, **46**, 2203–2205.
25 S. Lee, J. H. Nam, Y. J. Kim, Y. J. Cho, N. H. Kwon, J. Y. Lee, H. J. Kang, H. T. Kim, H. M. Park, S. Kim and J. Kim, *Macromol. Res.*, 2011, **19**, 827–834.
26 L. Zhao, C. Xiao, J. Ding, P. He, Z. Tang, X. Pang, X. Zhuang and X. Chen, *Acta Biomater.*, 2013, **9**, 6535–6543.
27 L. Zhao, J. Ding, C. Xiao, P. He, Z. Tang, X. Pang, X. Zhuang and X. Chen, *J. Mater. Chem.*, 2012, **22**, 12319–12328.
28 Y. Wang, X. Zhang, Y. Han, C. Cheng and C. Li, *Carbohydr. Polym.*, 2012, **89**, 124–131.
29 Q. Guo, Z. Wu, X. Zhang, L. Sun and C. Li, *Soft Matter*, 2014, **10**, 911–920.
30 M. J. Zhang, W. Wang, R. Xie, X. J. Ju, L. Liu, Y. Y. Gu and L. Y. Chu, *Soft Matter*, 2013, **9**, 4150–4159.
31 Y. Zhang, Y. Guan and S. Zhou, *Biomacromolecules*, 2006, **7**, 3196–3201.
32 Y. Zhang, Y. Guan and S. Zhou, *Biomacromolecules*, 2007, **8**, 3842–3847.
33 Y. Zhao, B. G. Trewyn, I. I. Slowing and V. S. Lin, *J. Am. Chem. Soc.*, 2009, **131**, 8398–8400.
34 L. Sun, X. Zhang, C. Zheng, Z. Wu and C. Li, *J. Phys. Chem. B*, 2013, **117**, 3852–3860.
35 F. Shi, J. Ding, C. Xiao, X. Zhuang, C. He, L. Chen and X. Chen, *J. Mater. Chem.*, 2012, **22**, 14168–14179.
36 H. Y. Tian, C. Deng, H. Lin, J. Sun, M. Deng, X. Chen and X. Jing, *Biomaterials*, 2005, **26**, 4209–4217.
37 J. V. Gonzalez-Aramundiz, M. V. Lozano, A. Sousa-Herves, E. Fernandez-Megia and N. Csaba, *Expert Opin. Drug Deliv.*, 2012, **9**, 183–201.
38 J. Ding, F. Shi, C. Xiao, L. Lin, L. Chen, C. He, X. Zhuang and X. Chen, *Polym. Chem.*, 2011, **2**, 2857–2864.
39 J. Ding, L. Zhao, D. Li, C. Xiao, X. Zhuang and X. Chen, *Polym. Chem.*, 2013, **4**, 3345–3356.
40 A. C. Engler, A. Shukla, S. Puranam, H. G. Buss, N. Jreige and P. T. Hammond, *Biomacromolecules*, 2011, **12**, 1666–1674.
41 A. R. Song, A. A. Rane and K. L. Christman, *Acta Biomater.*, 2012, **8**, 41–50.
42 T. J. Deming, *Prog. Polym. Sci.*, 2007, **32**, 858–875.
43 D. L. Nettles, A. Chilkoti and L. A. Setton, *Adv. Drug Deliv. Rev.*, 2010, **62**, 1479–1485.
44 G. Liu, R. Ma, J. Ren, Z. Li, H. Zhang, Z. Zhang, Y. An and L. Shi, *Soft Matter*, 2013, **9**, 1636 – 1644.
45 C. Xiao, C. Zhao, P. He, Z. Tang, X. Chen and X. Jing, *Macromol. Rapid Comm.*, 2010, **31**, 991–997.
46 J. Ding, X. Zhuang, C. Xiao, Y. Cheng, L. Zhao, C. He, Z. Tang and X. Chen, *J. Mater. Chem.*, 2011, **21**, 11383–11391.
47 Y. S. Lin and C. L. Haynes, *J. Am. Chem. Soc.*, 2010, **132**, 4834–4842.
48 Y. X. Wang, X. G. Zhang, Y. C. Han, C. Cheng and C. X. Li, *Carbohydr. Polym.*, 2012, **89**, 124–131.
49 R. J. Ma, H. Yang, Z. Li, G. Liu, X. C. Sun, X. J. Liu, Y. L. An and L. Q. Shi, *Biomacromolecules*, 2012, **13**, 3409–3417.
50 H. Yao, F. Chang and N. Hu, *Electrochim. Acta*, 2010, **55**, 9185–9192.
51 S. H. Brewer, A. M. Allen, S. E. Lappi, T. L. Chasse, K. A. Briggman, C. B. Gorman and S. Franzen, *Langmuir*, 2004, **20**, 5512–5520.
52 R. Narayanan and M. A. El-Sayed, *J. Phys. Chem. B*, 2005, **109**, 4357–4360.
53 H. Chen, M. Lee, J. Lee, J. H. Kim, Y. S. Gal, Y. H. Hwang, W. G. An and K. Koh, *Sensors*, 2007, **7**, 1480–1495.
54 B. Wang, R. Ma, G. Liu, Y. Li, X. Liu, Y. An and L. Shi, *Langmuir*, 2009, **25**, 12522–12528.
55 X. Jin, X. Zhang, Z. Wu, D. Teng, X. Zhang, Y. Wang, Z. Wang and C. Li, *Biomacromolecules*, 2009, **10**, 1337–1345.

Colour graphic

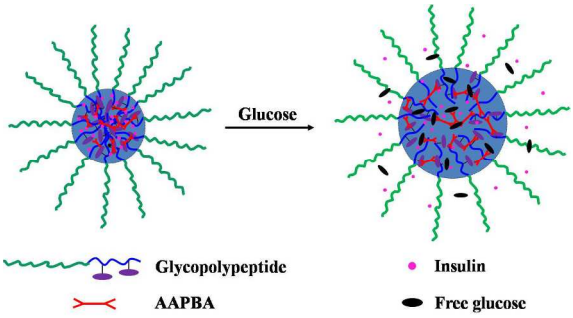

Text

A novel core cross-linked glycopolypeptide nanogel was prepared for glucose-triggered insulin delivery.